JJEE
Volume 6, Number 3, 2020
Pages 237-252
Jordan Journal of Electrical Engineering
ISSN (Print): 2409-9600, ISSN (Online): 2409-9619

# Electrodes for Alkaline Water Electrolysers with Triangle Shape Topology

**María J. Lavorante[1]*, Rodrigo Diaz Bessone[2], Samanta Saiquita[3], Gerardo M. Imbrioscia[4], Erica Ramirez Martinez[5]**

[1, 2, 3, 4] Institute of Scientific and Technological Research for Defense, Buenos Aires, Argentina
E-mail: mlavorante@citedef.gob.ar
[1, 5]Army Engineering Faculty, Div. Grl. Manuel Nicolas Savio (FIE), Buenos Aires, Argentina

*Received: March 11, 2020* *Revised: April 25, 2020* *Accepted: May 10, 2020*

***Abstract*—** Hydrogen is an energy carrier that is used in a wide variety of applications, including generation of a clean energy by fuel cells and as a fuel in vehicles. This leads to mitigating the negative impacts of utilizing fossil fuels in such applications. Water electrolysers are crucial devices for hydrogen production. However, they suffer from low rate of gas evolution and high energy consumption. In this paper, in order to tackle these two issues, we propose 316L stainless steel electrodes – which we created - with a triangle shape topology for alkaline water electrolysers. The electrodes' triangle topology is formed using electroerosion that allowed obtaining an average surface roughness of 12.6 µm. The performance of the proposed electrolyzer is investigated with six different values of the distance between electrodes, namely 8.2, 6.05, 5.4, 4.2, 3.7 and 1.6 mm at two values of operating temperature (20.1 and 30 °C). The obtained polarization curves per unit area (current density versus applied voltage) show that as the distance between electrodes is decreased, the current density increases due to the decrease in the electrical resistance. A higher current density implies a greater quantity of the formed product. Thus, using the same amount of energy, a greater volume of hydrogen is obtained. The results of investigating the effect of the operating temperature on the electrolyser's performance disclose that – contrary to the effect of the distance between electrodes - the current density increases with the increase in the operating temperature, yielding a higher rate of hydrogen evolution. Moreover, the results revel that the optimal performance of the electrolyser - when considering the combined effect of the operating temperature and the distance between electrodes - is achieved: i) at a distance of 2.6 mm and an operating temperature of 30 °C; and ii) at a distance of 1.6 mm between electrodes and 20.1 °C operating temperature.

***Keywords*—** Alkaline water electrolyser; Triangle shape topology; Electrodes; Hydrogen; Energy.

## 1. INTRODUCTION

Hydrogen technology plans to establish the use of hydrogen as an energy carrier to avoid or to reduce carbon dioxide ($CO_2$) emissions resulting from the utilization of fossil fuels. It also aims to modify the present energy system to one that can integrate hydrogen with fuel cells that transform the chemical energy of hydrogen into electricity and heat [1-3].

Hydrogen presents the highest energy content per mass. The combustion between hydrogen and oxygen follows the chemical reaction:

$$2H_2 + O_2 \rightarrow 2H_2O + \Delta H \quad (1)$$

where $\Delta H$ is the enthalpy of the combustion product that has a higher heating value (HHV) of 142.18 MJ/kg and a lower heating value (LHV) of 120.21 MJ/kg. This allows considering it as the best "clean" alternative to the fossil fuels since when it is burned together with oxygen, it generates only water as vapor and, consequently, the LHV represents the amount of energy usable to do work. Since it has a very small density, hydrogen has the lowest energy density of all combustion fuels: LHV of 10.074 MJ/m$^3$ and HHV of 11.915 MJ/m$^3$ [4, 5].

* Corresponding author
Article's DOI: 10.5455/jjee.204-1590965088

Many various methods are used for the obtention of hydrogen. They include [6-9]:

- Artificial photosynthesis.
- Bio-photolysis.
- Coal gasification.
- Dark fermentation.
- Electrolysis.
- Fossil fuel reforming: steam reforming, partial oxidation and auto-thermal reforming.
- High temperature electrolysis.
- Hybrid thermochemical electrolysis.
- Plasma arc decomposition.
- PV electrolysis.
- Photocatalysis.
- Photoelectrochemical method.
- Photofermentation.
- Photoelectrolysis.
- Thermolysis.
- Thermochemical processes: biomass conversion, gasification, reforming and water splitting.

But hydrogen should be produced through processes that use renewable resources to completely avoid $CO_2$ emissions. Unfortunately, renewable energies suffer from their regionalism, intermittency and unsustainability that cause instability of the energy source.

On the other hand, water electrolysis - as a method for hydrogen production - has the following advantages over the aforementioned methods: its simplicity, use of different energy sources for its operation, non-pollutant when used with renewable sources and purity - to a high degree - of its products. However, only 4% of the world's hydrogen production utilizes this method, especially when a high degree of purity is required [10-13]. The hydrogen produced by this process is considered the best energy carrier because it provides a balance between the generation of energy from renewable resources and its final use.

Water electrolysers can play a very important role in the distributed production of energy, its conversion, storage and use. They carry out two important functions: the first one is the production of hydrogen, and the second – that arises as a consequence of the first – is the energy storage. The latter occurs at times when there is high availability of renewable energy, which can be stored in the form of hydrogen for further utilization and can be transported to regions where there is a lack of renewable or insufficient resources to provide energy for industries, electric stations or domestic consumers [14-22].

The problems resulting from utilizing the water electrolysers are the low rate of evolution of gases and high energy consumption. Generally, the energy requirements for the industrial electrolysers are between 4.5 and 5 kWh $m_n^{-3}$ $H_2$ [23-25]. This means that the hydrogen cost is directly proportional to the energy, used to operate the electrolysers at a significant current density. In order to reduce energy consumption and consequently to satisfy the requirements for a sustainable hydrogen production, it is very important to enhance the process in terms of energy efficiency, safety, useful life, operability, portability and reduction of operation and maintenance costs.

A very important parameter to represent the energy consumption in water electrolysers is the cell voltage ($V_C$). The thermodynamic voltage of water decomposition has a value of 1.23 V. According to Faraday's, law the quantity of electricity (Q) necessary to produce 1 mol of $H_2$ under standard conditions is 2 F. Therefore, the theoretical energy ($W_T$) required to produce 1 $m^3$ $H_2$ is [26]:

$$W_T = V_C * Q = 2.94 \text{ kWh}/m^3 H_2 \quad (2)$$

The amount of electricity is equal to:

$$Q = I * t \quad (3)$$

where I is the current intensity in amperes [A] and t is the time in seconds [s]; therefore, Q is in coulombs [C].

But in industrial electrolysers, the cell voltage is between 1.8 and 2.6 V and these values are a consequence of high overpotential and large ohmic voltage drop. If the minimum and maximum values are averaged, the cell voltage will be 2.2 V, for which the experimental energy consumption ($W_e$) is 5.26 kWh/$m^3$ $H_2$. The energy efficiency ($\eta_e$) of the water electrolysis for the production of hydrogen is given by:

$$\eta_e = (W_t/W_e) * 100\ \% = 55.9\ \% \quad (4)$$

This highlights the imperative need to improve the process by the efficient use of the renewable resources. It also implies that to carry out the process, the following barriers must be overcome: the electrical resistances of the electric circuit; the activation energies of the electrochemical reactions of hydrogen and oxygen evolution that occur on the electrodes' surface; the availability of the electrodes' surface that may be partially covered by the formed gaseous products and the resistances for the ionic transport inside the electrolytic solution.

Overcoming all of these barriers is achieved by having a sufficient supply of electrical energy. The total resistance representing these barriers is given by [10]:

$$R_T = R_{EECA} + R_A + R_{OB} + R_M + R_I + R_{HB} + R_C + R_{EECC} \quad (5)$$

where $R_T$ is the total resistance, $R_{EECA}$ is the external electrical resistance of the anodic compartment circuit, $R_A$ is the over potential of the oxygen evolution reaction, $R_{OB}$ is the resistance caused by the partial covering of the electrode surface by the oxygen bubbles, $R_M$ is the resistance of the membrane, and $R_I$ is the resistance of the electrolyte. Other resistances correspond to the partial covering of the surface of the electrode by the hydrogen bubbles ($R_{HB}$) is the overpotential of the evolution reaction of hydrogen ($R_C$) and the external electrical resistance of the cathodic compartment circuit ($R_{EECC}$).

The topic of the present research work has been subjected to investigation by many authors. In an experimental work conducted by Ahn et al. [27], different morphological designs of electrodeposited Ni catalysts were presented in order to decrease the oxygen evolution reaction (OER) overpotential by enhancing the detachment of bubbles. On a glassy carbon substrate, the deposition Ni catalysts were controlled by potential and time. The following different morphologies were analyzed (with their deposition parameters in parentheses): flat (from Sigma Aldrich); smooth (-1.20 V for 20 s); cauliflower-like (-1.00 V for 60 s) and needle-like (-0.80 V for 180 s). In that order, the surface roughness increased after atomic force microscopy (AFM) analysis. A more hierarchical morphology was obtained as the potential became more positive. From contact angles of water droplets determination, it could be established that angle decreased as roughness increased. Previous studies on Ni surfaces showed - in a complete agreement with Wenzel's model [28] - that they became more hydrophilic as their roughness increased [29]. Results suggested that the more hierarchical the surface is, the smaller number of bubbles remain attached to it, implying shorter residence time and minor average size of oxygen bubbles on needle-like catalysts.

Fan et al., [30] characterized nickel-molybdenum, nickel-tungsten, cobalt-molybdenum and cobalt-tungsten cathodes for hydrogen evolution reaction (HER). In connection with HER overpotential, at low deposit loading range (approximately below 250 mg/cm$^2$), there was a rapid decline; however, at higher loadings (300-1200 mg/cm$^2$) that rate was reduced. It was found that among the analyzed electrodes, cobalt-molybdenum had the lowest values. It was also observed that the roughness tended, generally, to increase with increasing loadings. So, expanding the electrode surface decreases the overpotential. Regarding the electrode stability over time, the cobalt-molybdenum electrodes exhibited a stable performance. The nickel-molybdenum overpotential remained constant in the first 65 hours and then gradually began to increase. The results showed that the improvement in HER depends not only on the chemical composition of the electrodes but also on its active surface area, since increasing roughness decreases the overpotential.

Crnkonic et al., [31] prepared Ni-Fe-Mo co-deposits with and without the addition and subsequent leaching of zinc on mild steel substrates with the objective of maximizing their performance as cathode materials. From scanning electron microscope (SEM) images, it was concluded that the best method of obtaining the coating would be to add the zinc salt after avoiding disintegration of the coating after alkaline leaching or during equipment operation. From the steady-state polarization curves, it was determined that the most active is the coating to which zinc salt was added after 60 minutes. Molybdenum considerably improved the performance of the cathodes, when they were compared to that of bright Ni and showed that the incorporation and subsequent removal of zinc provides a very active material for HER. Finally, the stability of the cathodes was evaluated, evidencing a performance decline over time. SEM surface analysis showed a significant degradation of the Ni-Fe-Mo cathode, which may be due to the removal of molybdenum species that were in contact with hot alkali. In Ni-Fe-Mo-(Zn) remained on the surface in an appreciable amount and also exhibited a large electrochemical surface. Therefore, combination of properties such as surface area and intrinsic activity is a possible alternative to be used in the development of electrodes' material for water electrolysis.

In a study carried out by Lotfi et al. [32], the electrodeposition parameters of a Ni-Cu coating were optimized by means of the response surface methodology. Two Ni-Cu electrodes were synthesized: i) electrode A with high intrinsic response and ii) electrode B with high surface response. The dendritic structure that formed the Ni-Cu coating on nickel foam can improve the activity of HER because it has a larger active surface area. The electrode B had a higher porosity and showed better electrocatalytic activity than the electrode A which is attributed to its greater active surface area. It had the slightest charge transfer resistance and the greatest conductivity. Also, the B electrode presented the lowest values in release times and bubble size due to the following two facts: i) its sharp dendritic structure; if bubbles are detached faster, the surface exposed to the electrolyte increases to promote the reaction and ii) increasing the electrode/electrolyte interface improves the catalytic activity of the reaction; a smaller size decreases the adhesion forces of bubbles and the stability time of the electrocatalysis rises during the reaction process. The effect of the surface response over the properties of HER was greater than that of intrinsic ones.

Olivares-Ramirez et al. [33] studied three different types of stainless steel: 304; 316 and 430, to select the one with the best properties to be used as cathodes in sodium and

potassium hydroxide. Significant differences are observed between both electrolytes, especially in the area corresponding to the hydrogen adsorption-desorption. This behavior was attributed to the fact that nickel has a great tendency to adsorb hydrogen atoms in NaOH to form metallic hydrides of a not well-defined composition. Hydride formation occurs simultaneously with HER and has been reported in amorphous [34, 35], crystalline [36, 37] and composite nickel electrodes. 316 stainless steel was the best material as it produces the same volume of hydrogen in less time. This fact was accredited to nickel content of 12% in comparison with the other evaluated steels (304: 9.25% and 430: 0.75%). The use of KOH is encouraged since HER is more efficient because formation of hydrides is minimal and it is less corrosive to these types of materials [33].

In the work of Nagai et al. [38], the effect of bubbles on the performance of water electrolysis was analyzed using Ni-Cr-Fe alloy electrodes. The results showed two different behaviors depending on current density. At low current densities (0.1 to 0.5 $A/cm^2$), the voltage decreased as the distance between electrodes became smaller. When that value of current densities was exceeded (becoming ≤ 0.9 $A/cm^2$), the voltage increased slightly when the distance reached the region of 1-2 mm. As the distance between electrodes became smaller, the electrical resistance decreased, while the void fraction became quite small. For higher densities with small distance between electrodes, the void fraction became larger and this caused an increase in the electrical resistance and therefore, decreased the electrolysis's efficiency.

In order to decrease the energy consumption required to produce a certain mass flow of hydrogen, we created and investigated the performance of electrodes with triangle shape topology for alkaline water electrolyser.

## 2. MATERIALS AND METHODS

### 2.1. Electrodes Preparation

Stainless Steel 316L is the material selected for the electrodes because of its 12% nickel content [33]. There is one pair of electrodes; its dimensions are 110x110x3 mm. Scheme for the triangle shape topology is shown in Fig. 1(a). In Fig. 1(b), two sectors can be seen: the channel or groove (in the form of painted triangles) and the rib. Electroerosion is method used to engrave the geometry on the surface of the electrodes as it allows obtaining different roughness grades, which is a point of interest in this type of systems. So, as a first step, it is necessary to build a copper electrode with the corresponding geometry and later using it in the electroerosion machine.

The electroerosion machine is provided with a "profile-meter" which allows selecting or determining the surface finish by comparison. The scale is defined in Charmilles "CH" which is provided to compare commonly used standards such as Ra (Europe) – CLA (UK) – AA (USA) [39]. The roughness for the pair of electrodes is CH42. Charmilles has designated a CH scale which is cross referenced with the standards that are in common use as roughness average (Ra) [40]. Ra is obtained by an algorithm that measures the average length between valleys and peaks and the deviation from the mean line on the entire surface within the sampling length [41, 42]. CH42 is equivalent to 12.6 μm Ra.

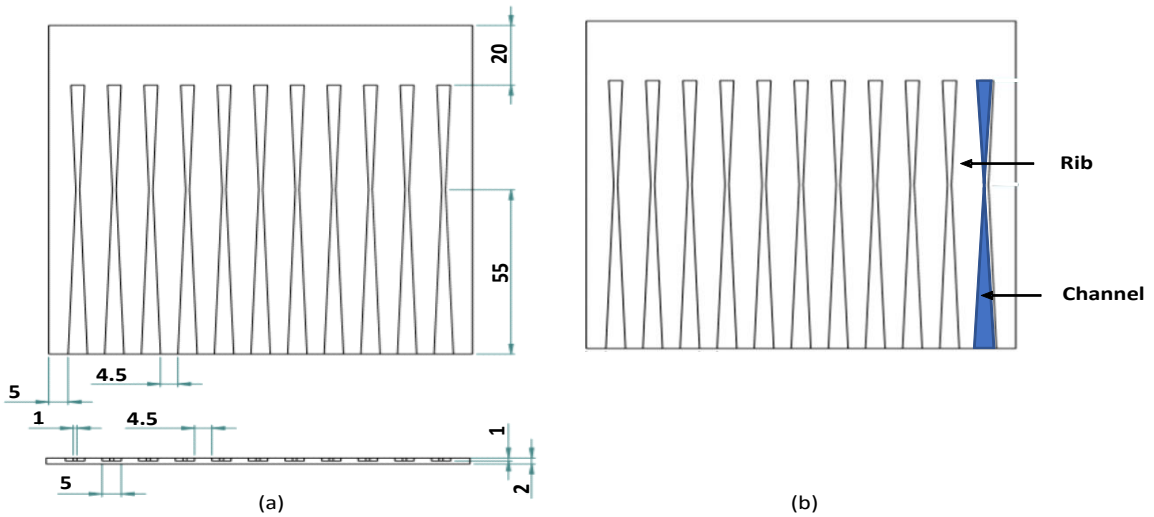


Fig. 1. a) View of the electrode with triangle shape topology; b) electrode zones: channel and rib.

Once the electrodes have been built, they have to be cleaned with the objective to eliminate the impurities left by machining and the manipulation of the pieces. As a first stage, an abrasive cleaner is used. It is composed of sodium dodecylbenzene sulfonate, carbonates and alkalinizing agent. Afterwards, the electrode is washed under tap water and, finally, it is rinsed with distilled water. As a final step, once the electrode is dry, a piece of filter paper is soaked with acetone (Sintorgan® Pro-Analysis) and used to clean the surface and then it is left to dry.

In order to analyze the roughness on the electrodes, a SEM, Philip SEM 515, is used to produce high resolution images of the triangle shape channels.

## 2.2. Preparation of the Electrode Evaluation Cell

To analyze the effect of the distance between electrodes and the proposed topology, the evaluation cell needs to be put together. The electrode evaluation cell consists of:

a) A cubic container
b) Six pairs of gauges
c) Two guide brackets
d) Two mobile locks.

All pieces are constructed in crystal acrylic, except for the screws used to bond and hold some of the mobile pieces. The electrode evaluation cell is composed of a main body corresponding to a container, within which all the previously mentioned components are placed in addition to a physical separator or diaphragm, the electrolyte and the electrodes. For the physical separator to be in a perfectly parallel position at the same distance from both electrodes, a channel or groove is positioned in the center along its walls and base. The purpose of this channel is to: i) easily place the separator ensuring its vertical and parallel position to the electrodes and ii) act as the structural frame of the selected diaphragm. The material used as separator is Zirfon Perl UTP 500 by Agfa, which is an open mesh polyphenylene sulphide fabric, symmetrically coated with a polymer and zirconium oxide particles [43, 44]. The electrolyte is a 30% m/m potassium hydroxide (Biopack 85.0%) solution.

Inside the container, the electrolyte is placed first and afterwards the separator. There are six different pairs of gauges, which - depending on their size - allow establishing the desired distance between electrodes. They are placed at both sides of the separators and the guide brackets are positioned over them as shown in Fig. 2.

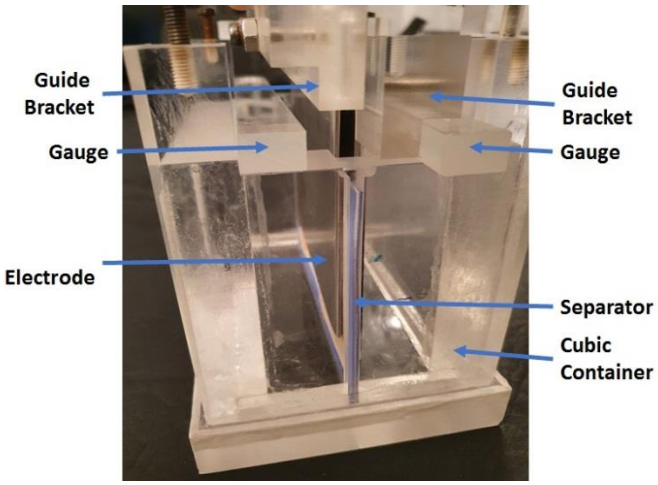


Fig. 2. Position of the electrode evaluation cell's components.

Prior to placing the electrodes inside the cubic container, the electrodes are situated over a support piece (guide brackets). This keeps them parallel and equidistant from each other and from the separator. The electrodes are attached to these pieces by stainless-steel screws. The guide brackets have a notch that allows them to rest on the gauges and in this way establish the distance that is the object of analysis. The mobile block ensures the position of the guide brackets and the gauges throughout the entire study and maintains the distance between electrodes as shown in Fig. 3.

Once the electrode evaluation cell is assembled, the electrodes are connected directly to the power supply TDK-Lambda 12.5 V/60 A through copper wires. After this, it is corroborated that all the components are in place, the mobile brackets are fixed and the real distance between electrodes is determined. It must be taken into consideration that the distance is reached by the configuration of the gauges and the thickness of the plates being used as electrodes.

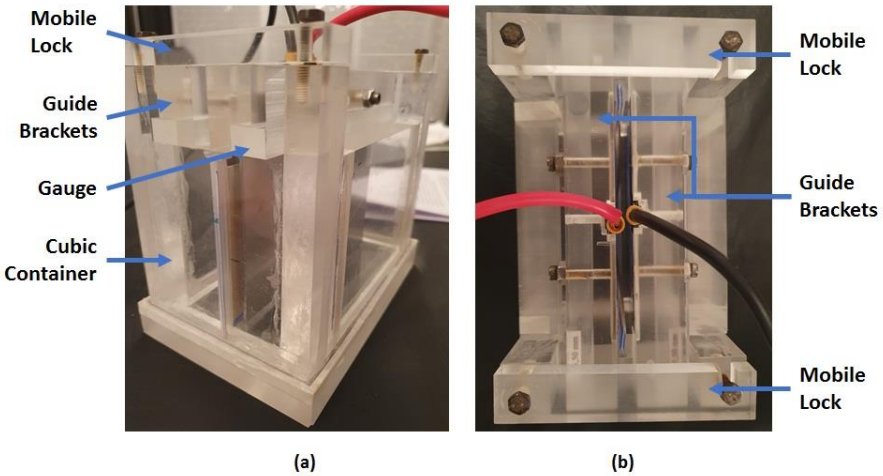


Fig. 3. The electrode evaluation cell: a) View of the body; b) upper part.

As the initial operating temperature is established, the system is brought to the defined operating temperature, setting the system into operation. Once the temperature is reached, the experiment is initiated. The potential difference varies by 0.1 V every 30 s along applied voltage ranging from 0 to 2.4 V or from 0 to 3 V.

Analysis of each investigated distance is performed at least four times if no unexpected variation of the results is found. If this occurs, the analysis would be executed 4 extra times, for the detection of the possible cause and the discard of the wrong series of results. The analysis includes the calculation of the standard deviation and the corresponding relative error. Table 1 shows the operating parameters studied for the surface finish, CH42.

Table 1. The investigated operating conditions: distance between electrodes and temperature.

| Electrodes | Temperature [$^{o}$C] | Distance between electrodes [mm] | | | | | |
|---|---|---|---|---|---|---|---|
| CH42 | 30 | 8.10 | 8.00 | 6.05 | 5.20 | 4.20 | 2.60 |
| CH42 | 20.1 | 8.20 | 6.05 | 5.40 | 4.20 | 3.70 | 1.60 |

Some of the experiments are also carried out at different initial operating temperatures, namely: 20.1 °C and 30 $^{o}$C. Assembly of the cell, the execution of experiments and the record and evaluation of the results are performed in the same way.

## 3. RESULTS AND DISCUSSION

### 3.1. Evaluation of the Surface Area

Since the electrode surface acts as a catalyst, the type and reaction rate rely on the specific interactions between the ionic species that conform the electrolyte and the electrodes surface, making it more appropriate roughness surface. A surface with these characteristics can favor an increase over the electrocatalytic activity of the selected material.

The idea of utilizing the proposed triangle shape geometry – shown in Fig. 1(a) - is to facilitate the detachment of the bubbles formed through the reduction of the channel width in the lower portion and the orientation to the upper part. Additionally, there is a surface that is rougher (the channel area) than the other (the rib area) as shown in Fig. 1(b). The bubbles - generated in the channel's area - can meet the channel's throttling when detached and this could favor them to move away from the surface more quickly and to drag other bubbles with them; thus, making the surface available.

The triangle shape topology was obtained by the use of electrical discharges. The surplus material is removed from the workpiece electrode by current discharges between two electrodes (the tool and the workpiece electrodes) which are separated by a dielectric liquid and are subdued to an electric voltage.

The obtained SEM images for the studied electrodes are shown in Fig. 4. It should be noted that the surface under study is the area inside the triangle channels. The images do not show the unmodified surface of the flat electrode. Fig. 4 presents the CH42 channel surface electrode. Two zones can be clearly distinguished: a 100x rough zone (see Fig. 4(a)) and a 100x smoother one (see Fig. 4(c)). The rougher area has discontinuities: there are pores, protuberances, and unevenness of different types and sizes. On the other hand, the smoother zone is more even without so many imperfections on its surface.

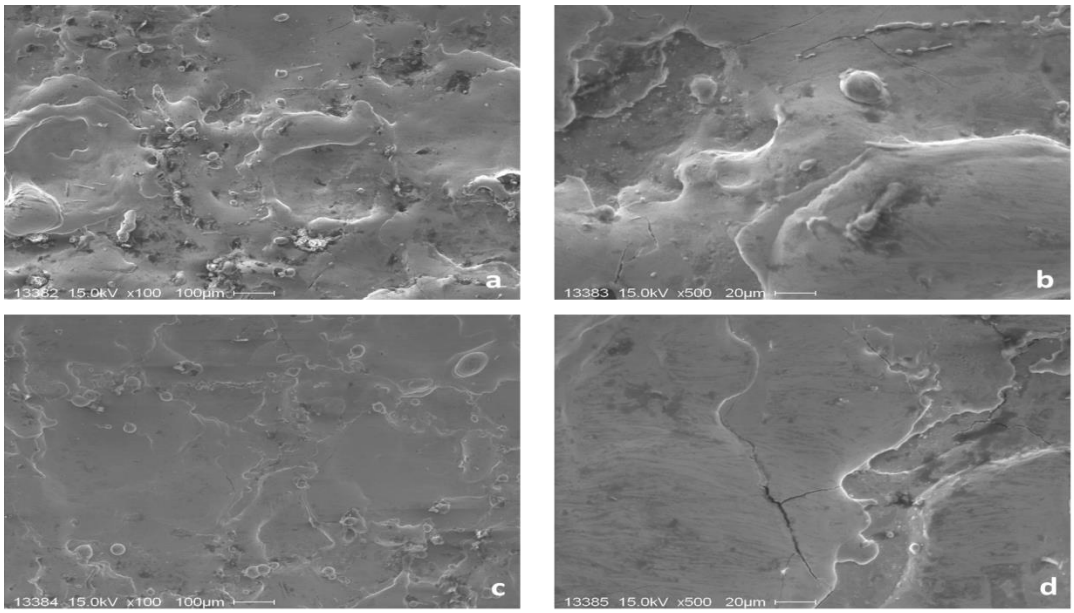


Fig. 4. SEM images of surface channel in CH42 electrode: a) 100 x rough zone; b) 500 x rough zone; c) 100 x smooth zone; d) 500 x smooth zone.

Figs. 4(b) and (d) show 500x rough and 500x smooth zones, respectively. In these figures, the rough zone presents a more tortuous surface with valleys and hills of different sizes and small globular-looking lumps that appear without following a defined pattern or dimension, while in the smooth zone, the presence of cracks or grooves and unevenness can be seen in more detail, although there is a notable predominance of a flat surface. This situation - may when analyzed as a whole - improve, worsen or not present a change in the performance of the system, rather than that achieved by increasing the surface of the electrode by incorporating the channel.

### 3.2. Effect of the Distance between Electrodes

In this section the polarization curves of CH42 electrodes are presented and the effect of distance between electrodes is evaluated. It should be clear that since the distances are obtained by the rectified acrylic blocks, it is difficult to follow a pattern, except for those arising from the combination of the size of the blocks and the thickness of the electrodes. To facilitate the analysis of the obtained data, the distances were divided into two groups: the first one comprises distances between 5 and 10 mm, and the second comprises distances smaller than 5 mm.

Using the data about currents obtained after applying various voltage values, the current densities were calculated. Fig. 5 presents the results for each of the investigated distances between electrodes. Figs. 5(a) and (b) show the polarization curves of the distances: (8.2, 6.05 and 5.4 mm) and (4.2; 3.7 and 1.6 mm), respectively at an initial operating temperature of 20.1°C. Figs. 5(c) and (d) show the polarization curves of the distances: (8.1, 8, 6.05 and 5.2 mm) and (4.2 and 2.6 mm), respectively with the initial operating temperature of 30 °C.

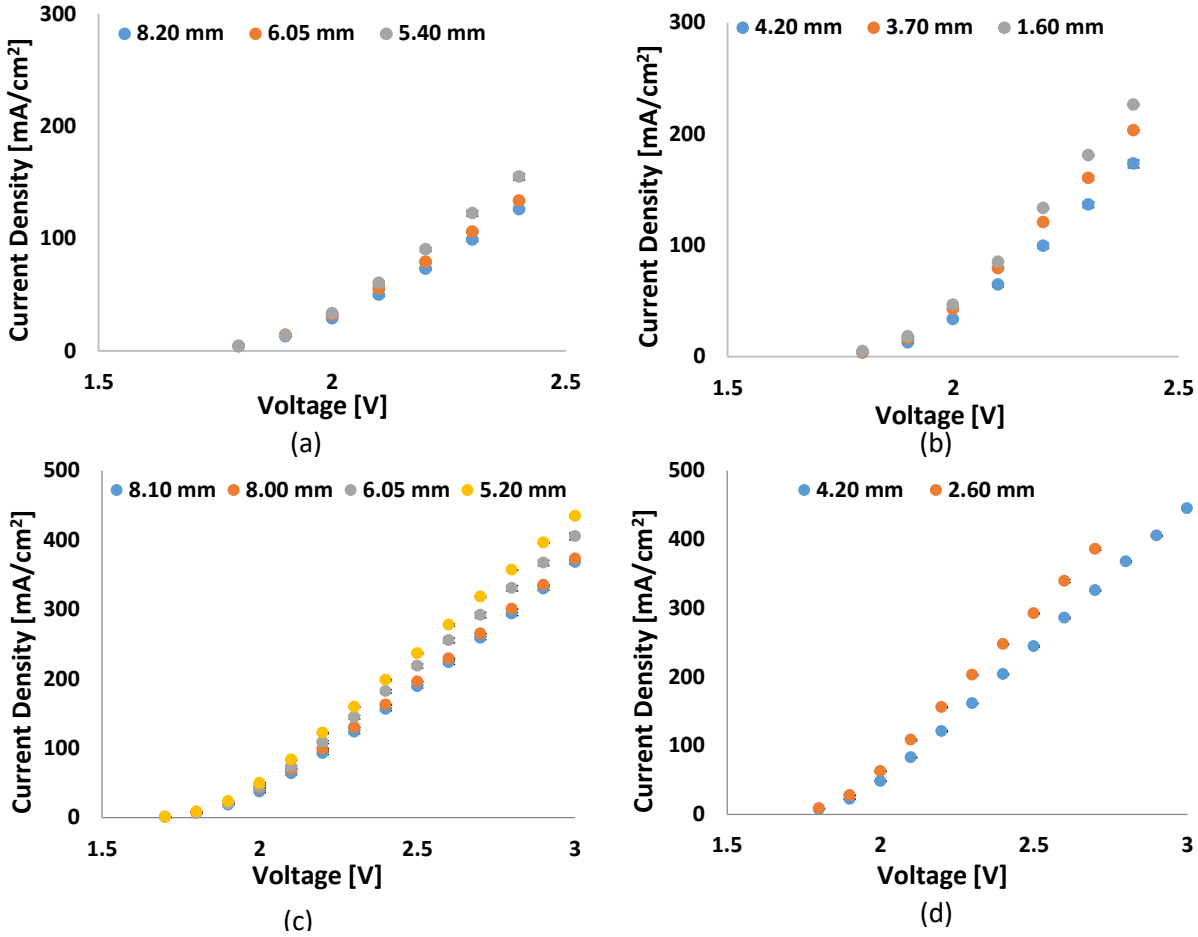


Fig. 5. Polarization curves per unit area (current density versus applied voltage): a) for 8.2, 6.05 and 5.4 mm distances between electrodes at 20.1 °C ; b) 4.2, 3.7 and 1.6 mm distances between electrodes at 20.1 °C; c) 8.1, 8, 6.05 and 5.2 mm distances between electrodes at 30 °C; d) 4.2 and 2.6 mm distances between electrodes at 30 °C.

The standard error for each point, which makes up the polarization curves, is plotted. Unfortunately, as the values are so small, it cannot be appreciated. The obtained average standard deviation is about 2.6 within the determinations at 20.1 °C and 2.75 at 30 °C. The average standard errors are approximately 1.3 and 1.35, respectively.

Fig. 5 shows that as the distance between electrodes is decreased, the current density increases. The best performance of the system is obtained at a distance between electrodes of 1.6 mm at 20.1°C and 2.6 mm at 30 °C, since the electrical resistance decreases as the distance becomes smaller. Nagai et al. [38] research work studied the effects of the distance between electrodes and current density of Inconel 600 electrodes. Although the operating conditions were different; other distances between electrodes, other operating voltages and other operating temperature, the effect on the performance of the system is similar. The voltage necessary to maintain a certain current density (between 100-500 mA/cm$^2$) was greater with the increased distances between electrodes.

In Figs. 6(a) and (c), the polarization curves obtained for the largest and closest distances between electrodes in both systems are exhibited. The gained improvement can be clearly appreciated. In Figs. 6(b) and (d), the percentage increase in the current density versus the applied voltage is represented. A higher current density implies a greater quantity of

formed product. Thus, by using the same amount of energy, a greater volume of hydrogen is obtained. From applying a voltage of 2.2 V to the system at 20.1 °C (see Fig. 6(b)), an increase of more than 80% is obtained and it goes down gradually along the applied voltage. In the case of 30 °C, as shown in Fig. 6(d), the maximum increase is observed with 2.1 V applied voltage with an approximate percentage increase in the current density of 70%, but then; the improvement is detrimental.

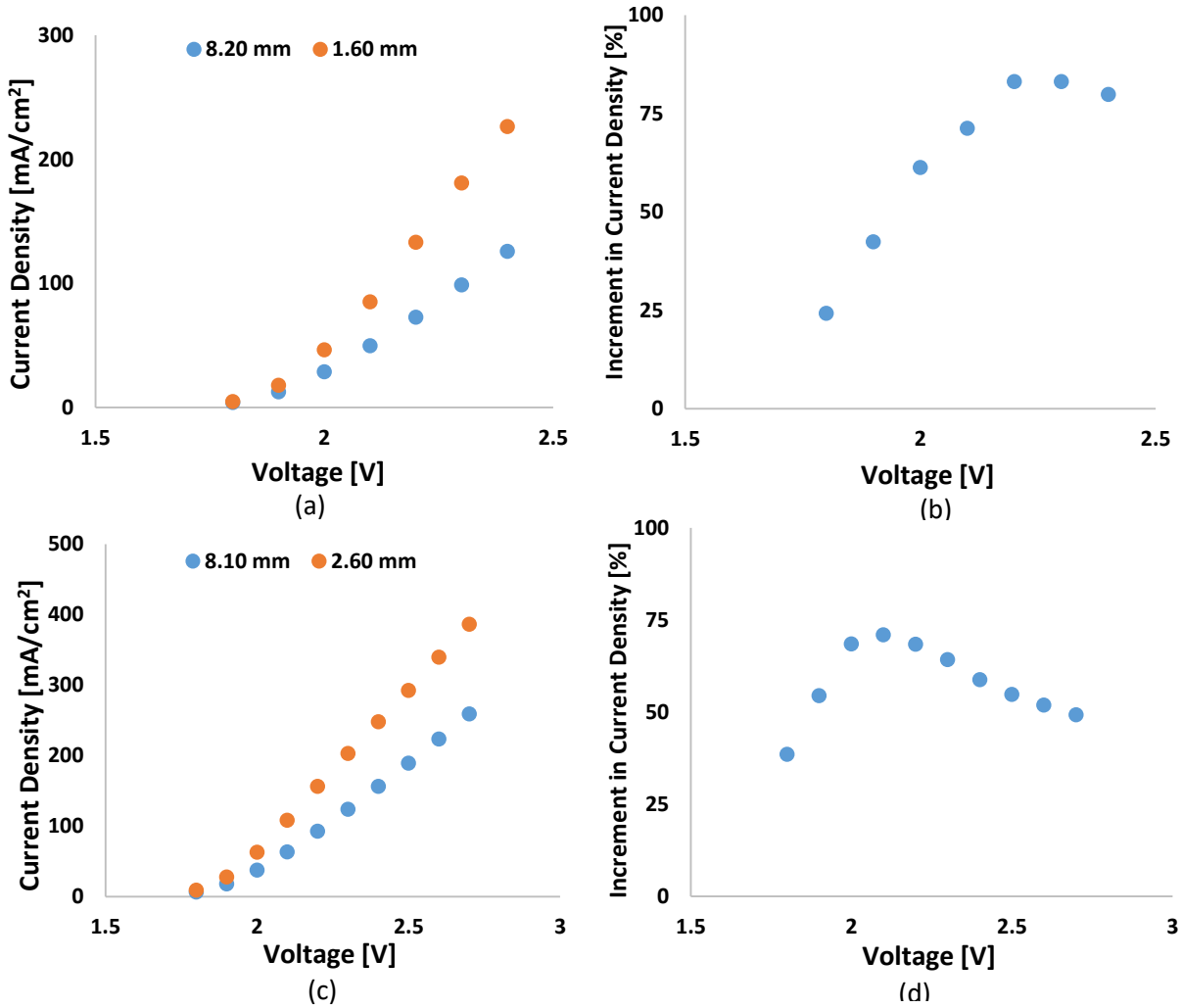


Fig. 6. a) Polarization curves of the electrodes for 8.2 mm and 1.6 mm distance between electrodes at 20.1 °C; b) percentage increase in the current density for the case a); c) polarization curves of the electrodes for 8.1 mm and 2.6 mm distance between electrodes at 30 °C; d) percentage increase in the current density for the case c).

The obtained results that are depicted on Fig. 6 indicate that at higher current densities, there is a greater amount of bubbles because the surface characteristics or the shape of the channel can make it difficult to detach bubbles properly. This - in some way - decreases the percentage of enhancing the system by increasing the applied voltage.

### 3.3. Effect of Temperature

To perform a detailed analysis, the behavior of the systems at different temperatures is investigated at two distances between electrodes, namely 6.05 and 4.20 mm (see Fig. 7). Fig. 7(a) shows the polarization curves with a distance of 6.05 mm at 20.1 and 30°C, and

Fig. 7(b) shows the percentage increase in the current density under the same conditions. In Figs. 7(c) and 7(d) exhibit the polarization curves with a distance of 4.2 mm at 20.1 and 30°C and the percentage increase in the current density under these conditions.

Fig. 7 reveals that the obtained current density increases with the increase in the initial operating temperature. However, that difference seems to decrease as the distance shortens. This could be associated with the greater amount of generated bubbles and with their release rate caused by the shape/geometry of the electrode itself.

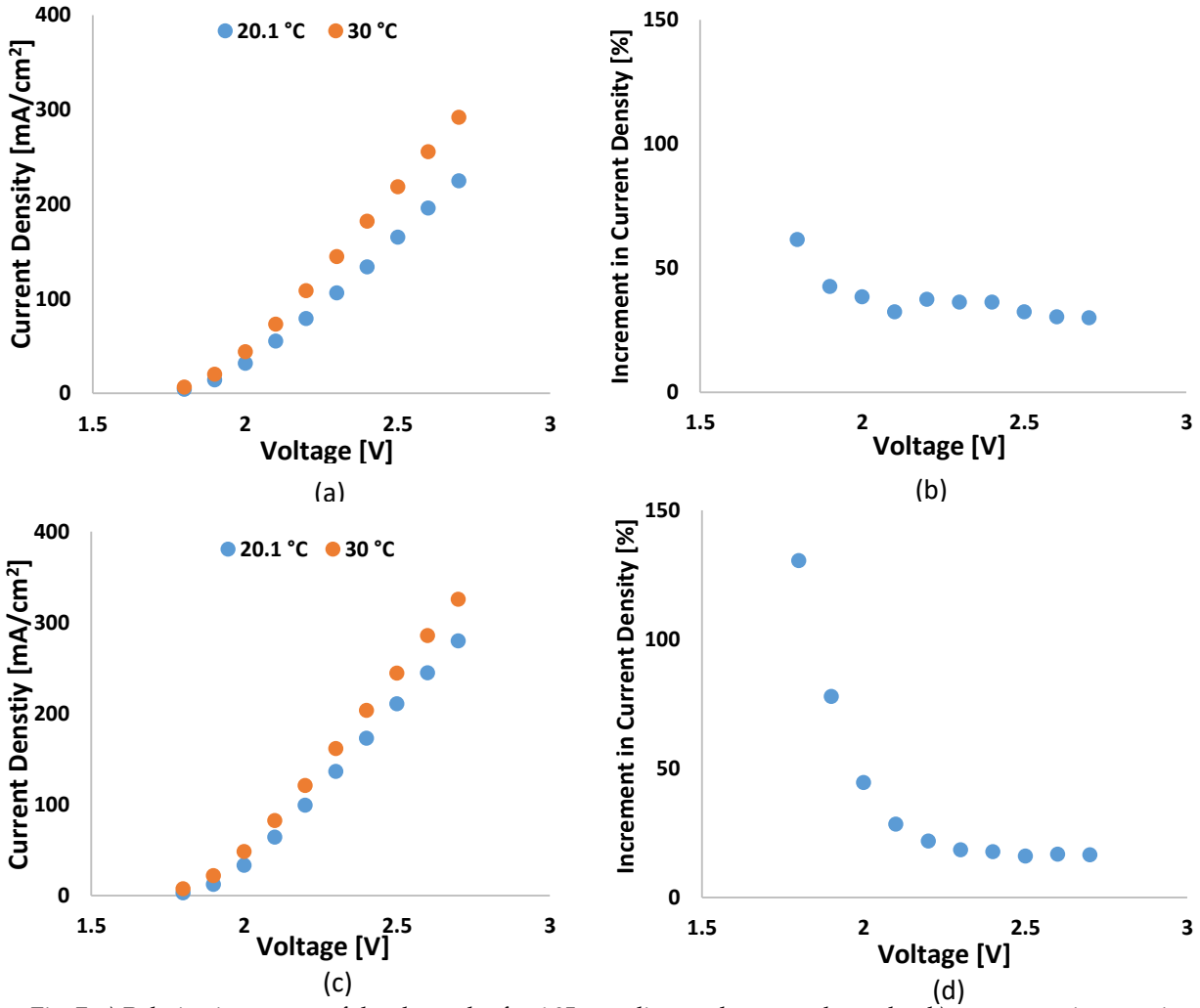


Fig. 7. a) Polarization curves of the electrodes for 6.05 mm distance between electrodes; b) percentage increase in the current density for the case a); c) polarization curves of the electrodes for 4.20 mm distance between electrodes; d) percentage increase in the current density for the case c).

Working at a higher initial temperature improves the efficiency of the system as well and comes in agreement with the results obtained by Nagai et. al [38]. This enhancement exceeds 60% at 6.05 mm and 100% at 4.20 mm as soon as the applied voltage for the water decomposition is reached, but it decreases rapidly until a plateau (of approximately 32% and 18%) between 2.3 to 2.7 V, respectively is attained.

The heat released by the system at a distance of 4.2 mm between electrodes is investigated. From Fig. 8, it can be noticed that for the same amount of generated hydrogen, the system releases more heat with the lowest performance, i.e. the system with an initial operating temperature of 20.1 °C. As the operating temperature increases, the electrolyte

inter-ionic attraction decreases since the electrolyte dissociation is greater as well as the number of involved ions in the conduction. This brings an ohmic drop in the electrolyte. This parameter is associated with ions flow rate between the electrodes and it is related to the current, the electrolyte conductivity and the distance between electrodes.

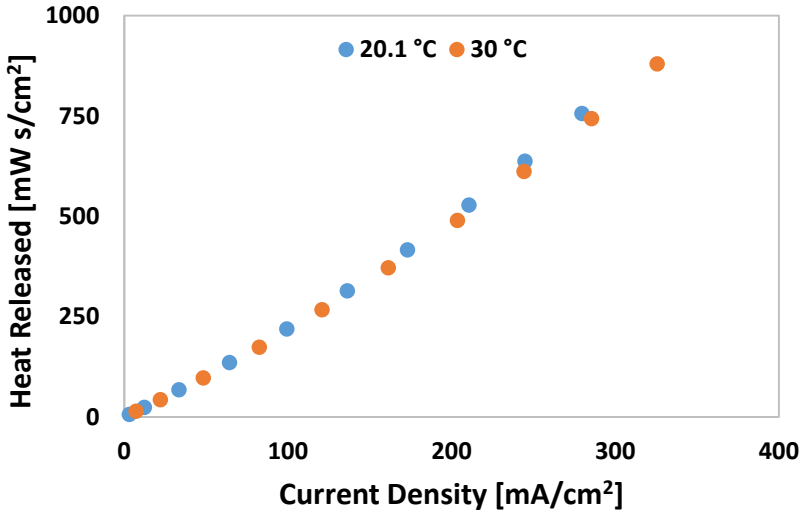


Fig. 8. Released heat as a function of the current density for a distance of 4.2 mm between electrodes.

Further research will be conducted in order to deepen the knowledge about the bubbles phenomena (formation and detachment) on these types of electrodes, as well as, analyzing the performance of the systems with different roughness in the channel zone.

## 4. CONCLUSIONS

The great challenge facing hydrogen's implementation as a fuel or energy carrier is the need to find new low-cost methods for its production or to reduce the current cost of the existing ones. Water electrolysers are crucial devices for hydrogen production. In order to reduce their energy consumption, cost and maintenance, electrolysers are operated with a renewable energy source. But making them operate steadily with the intermittent power of the renewable energy sources constitutes a challenge.

In order to improve the energy efficiency of water electrolysers and their performance, we created electrodes with a triangle shape topology for alkaline water electrolysers - using electrical discharge machining that allows obtaining different levels of CH42 surface roughness - and experimentally investigated their performance, namely the effect of both the temperature and the distance between electrodes on the elctrolyser's performance.

The results showed that the best performance was achieved at: i) a distance of 2.6 mm between electrodes at an operating temperature of 30 °C and ii) a distance of 1.6 mm between electrodes at an operating temperature of 20.1 °C. This clearly indicates that as the electrodes get closer and the distance between them smaller, the electrical resistance decreases along the analyzed distances. The electrical resistance is an important property of the structure and the material of the electrodes. It determines the size of the potential drop through the electrode which in succession contributes to the power costs, and can lead to energy waste in the form of heat and a less uniform potential distribution. A smaller distance between electrodes can

reduce resistance for ionic transportation. However, the optimal distance must be identified for each type of electrodes and diaphragm.

Operating the proposed system at higher temperature led to obtaining better performance and higher current density for each applied voltage. From a thermodynamics point of view, water dissociation by electrolysis required a theoretically minimum potential - the equilibrium voltage, below which the electrolysis cannot proceed. As the temperature was increased, the equilibrium voltage decreased. As the operating temperature was risen, the electrode reaction kinetics and the ion transport were accelerated. This means that the higher the temperature, the higher the reaction rate. Therefore, the higher the current density for the voltage applied, or the lower voltage requested for a certain current density.

The results of investigating the heat released by the system revealed that the system with a distance of 4.2 mm between electrodes at 20.1 °C released more heat to produce the same amount of hydrogen. So, the necessary electric power to produce a certain mass flow of hydrogen could be represented by the voltage.

Results of this work demonstrated that using the same voltage and modifying specific operating conditions, a greater production of hydrogen will be obtained.

Future work on the proposed electrodes' topology will focus on determining the type of interaction between surfaces obtained by the machining method in addition to bubbles' formation and detachment in the electrolysis process.

**Acknowledgement:** Authors wishes to thank the Argentinean Ministry of Defense and the Authorities of the Institute of Scientific and Technical Research for Defense (CITEDEF) for their support through the subsidy 03 NAC 024/17 granted to carry out this research. Our thanks extend to the Defense University, Army Engineering College for providing the power source used to carry out the investigations, to the staff of the CITEDEF's Prototype Department for the construction of the evaluated electrodes and to the staff of CITEDEF's Solid Research Division for the SEM micrographs.

## REFERENCES

[1] G. Marban, T. Valdes-Solis, "Towards the hydrogen economy?," *Intenational Journal of Hydrogen Energy*, vol. 32, no. 12, pp. 1625-1637, 2007.

[2] N. Muradov, T. Vezirolu, "From hydrocarbon to hydrogen? Carbon to hydrogen economy," *International Journal of Hydrogen* Energy, vol. 30, no. 3, pp. 225-237, 2005.

[3] S. Penner, "Steps toward the hydrogen economy," *Energy*, vol. 31, no. 1, pp. 33-43, 2006.

[4] X. Yan, R. Hino, *Nuclear Hydrogen Production Handbook*, Boca Raton: CRC Press, 2011.

[5] National Research Council and National Academy of Engineering, *The Hydrogen Economy: Opportunities, Costs, Barriers and R&D Needs*, Washington DC: The National Academies Press, 2004.

[6] I. Dincer, "Green methods for hydrogen production," *International Journal of Hydrogen Energy*, vol. 37, no. 2, pp. 1954-1971, 2012.

[7] I. Dincer, C. Acar, "Review and evaluation of hydrogen production methods for better sustainability," *International Journal of Hydrogen Energy*, vol. 40, no. 34, pp. 11094-11111, 2015.

[8] Y. Lang, R. Arnepalli, A. Tiwaril, "A review on hydrogen production: methods, materials and nanotechnology," *Journal of Nanoscience and Nanotechnology*, vol. 11, pp. 3719-3739, 2011.

[9] N. Brandon, E. Ruiz-Trejo, P. Boldrin, *Solid Oxide Fuel Cell Lifetime and Reliability: Critical Challenges in Fuel Cells*, Elsevier, Academic Press, 2017.

[10] M. Kaninski, D. Saponjic, I. Perovic, A. Maksic, V. Nikolic, "Electrochemical characterization of Ni-W catalyst formed in situ during alkaline electrolytic hydrogen production - part II ,"*Applied Catalysis A: General*, vol. 405, no. 1-2, pp. 29-35, 2011.

[11] A. Ursua, L. Gandia, P. Sanchis, "Hydrogen production from water electrolysis: current status and future trends," *Proceedings of the IEEE*, vol. 100, no. 2, pp. 410-426, 2012.

[12] M. Balat, "Potential importance of hydrogen as a future solution to environmental and transportation problems," *International Journal of Hydrogen Energy*, vol. 33, no. 15, pp. 4013-4029, 2008.

[13] K. Zeng, D. Zhang, "Recent progress in alkaline water electrolysis for hydrogen production and applications," *Progress in Energy and Combustion Science*, vol. 36, no. 3, pp. 307-326, 2010.

[14] P. Ghosh, B. Emonts, H. Janßen, J. Mergel, D. Stolten, "Ten years of operational experience with a hydrogen-based renewable energy supply system," *Solar Energy*, vol. 75, no. 6, pp. 469–478, 2003.

[15] S. Galli, M. Stefanoni, P. Borg, W. Brocke, J. Mergel, "Development and testing of a stand-alone small-size solar photovoltaic-hydrogen power system (SAPHYS)," *JOULE II-Programme, Directorate General XII: Science, Research and Development*, European Commission, Brussels, 1997.

[16] T. Schott, A. Siegel, *Advances in Solar Energy Technology: Volume 1*, Oxford: Pergamon Press, 1988.

[17] M. Little, M. Thomson, D. Infield, "Electrical integration of renewable energy into stand-alone power supplies incorporating hydrogen storage," *International Journal of Hydrogen Energy*, vol. 32, no. 10-11, pp. 1582-1588, 2007.

[18] E. Solomin, K. Kirpichnikova, R. Amerkhanov, D. Korobatov, M. Lutovats, A. Martyanov, "Wind-hydrogen standaolen uninterrupted power supply plant for all-climate application," *International Journal of Hydrogen Energy*, vol. 44, pp. 3433-3449, 2019.

[19] A. Kovac, D. Marcius, L. Budin, "Solar hydrogen production via alkaline water electrolysis," *International Journal of Hydrogen Energy*, vol. 44, no. 20, pp. 9841-9848, 2018.

[20] J. Romeo, N. Holmes, "BIG HIT to make Orkney a model hydrogen territory," *Fuel Cells Bulletin*, vol. 10, pp. 14-15, 2016.

[21] HYCHICO, *Clean Hydrogen Production and Renewable Energy Storage: An experience underway in Patagonia*, 2017. <https://4echile.cl/4echile/wp-content/uploads/2017/05/Clean-Hydrogen-Production-and-Renewable-Energy-Storage-ArielPerez-Hychico.pdf>

[22] P. Hollmuller, J-M. Joubert, B. Lachal, K. Yvon, "Evaluation of a 5 kWp photovoltaic hydrogen production and storage installation for a residential home in Switzerland," *International Journal of Hydrogen Energy*, vol. 25, pp. 97-109, 2000.

[23] D. Stojic, M. Marceta, S. Sovilj, S. Miljanic, "Hydrogen generation from water electrolyisis-possibilities of energy saving," *Journal of Power Sources*, vol. 118, no. 1-2, pp. 315-319, 2003.

[24] V. Nikolic, G. Tasic, A. Maksic, D. Saponjic, S. Miulovic, M. Marceta Kaninski, "Raising efficiency of hydrogen generation from alkaline water electrolysis – energy saving," *International Journal of Hydrogen Energy*, vol. 35, no. 22, pp. 12369-12373, 2010.

[25] S. Miulovic, S. Maslovara, M. Seovic, B. Radak, M. Marceta Kaninski, "Energy saving in electrolytic hydrogen production using Co-Cr activation – Part I," *International Journal of Hydrogen Energy*, vol. 37, no. 22, pp. 16770-16775, 2012.

[26] M. Wang, Z. Wang, X. Gong, Z. Guo, "The intensification technologies to water electrolysis for hydrogen production – A review," *Renewable and Sustainable Energy Reviews*, vol. 29, no. 3, pp. 573-588, 2014.

[27] S. Ahn, I. Choi, H. Park, S. Hwang, S. Yoo, E. Cho, H. Kim, D. Henkensmeier, S. Nam, S. Kim, J. Jang, "Effect of morphology of electrodeposited Ni catalysts on the behavior of bubbles generated during the oxygen evolution reaction in alkaline water electrolysis," *Chemical Communications*, vol. 49, no. 81, pp. 9323-9325, 2013.

[28] R. Wenzel, "Resistance of solid surfaces to wetting by water," *Industrial and Engineering Chemistry*, vol. 28, no. 8, pp. 988-994, 1936.

[29] S. Ahn, S. Hwang, S. Yoo, I. Choi, H. Kim, J. Jang, S. Nam, T. Lim, T. Lim, S. Kim, J. Kim, "Electrodeposited Ni dendrites with high activity and durability for hydrogen evolution reaction in alkaline water electrolysis," *Journal of Material Chemistry*, vol. 22, no. 30, pp. 15153-15159, 2012.

[30] C. Fan, D. Piron, A. Sleb, P. Paradis, "Study of electrodeposited nickel-molybdenum, nickel-tungsten, cobalt-molybdenum, and cobalt-tungsten as hydrogen electrodes in alkaline water electrolysis," *Journal of The Electrochemical Society*, vol. 141, no. 2, pp. 382-387, 1994.

[31] F. Crnkovic, S. Machado, L. Avaca, "Electrochemical and morphological studies of electrodeposited Ni–Fe–Mo–Zn alloys tailored for water electrolysis," *International Journal of Hydrogen Energy*, vol. 29, no. 3, pp. 249–254, 2004.

[32] N. Lotfi, T. Shahrabi, Y. Yaghoubinezhad, G. Darband, "Surface modification of Ni foam by the dendrite Ni-Cu electrode for hydrogen evolution reaction in an alkaline solution," *Journal of Electroanalytical Chemistry*, vol. 848, pp. 1-10, 2019.

[33] J. Olivares-Ramírez, M. Campos-Cornelio, J. Uribe Godínez, E. Borja-Arco, R. Castellanos, "Studies on the hydrogen evolution reaction on different stainless steels," *International Journal of Hydrogen Energy*, vol. 32, no. 15, pp. 3170–3173, 2007.

[34] L. Vračar, B. Conway, "Hydride formation at Ni-containing glassy-metal electrodes during the H2 evolution reaction in alkaline solutions," *Journal of Electroanalytical Chemistry and Interfacial Electrochemistry*, vol. 277, no. 1-2, pp. 253–275, 1990.

[35] L. Vračar, B. Conway, "Temperature dependence of electrocatalytic behaviour of some glassy transition metal alloys for cathodic hydrogen evolution in water electrolysis," *International Journal of Hydrogen Energy*, vol. 15, no. 10, pp. 701–713, 1990.

[36] B. Conway, H. Angerstein-Kozlowska, M. Sattar, B. Tilak, "Study of a decomposing hydride phase at nickel cathodes by measurement of open-circuit potential decay," *Journal of The Electrochemical Society*, vol. 130, no. 9, pp. 1825-1835,1983.

[37] D. Soares, O. Teschke, I. Torriani, "Hydride effect on the kinetics of the hydrogen evolution reaction on nickel cathodes in alkaline media," *Journal of The Electrochemical Society*, vol. 139, no. 1, pp. 98-104, 1992.

[38] N. Nagai, M. Takeuchi, T. Kimura, T. Oka, "Existence of optimum space between electrodes on hydrogen production by water electrolysis," *International Journal of Hydrogen Energy*, vol. 28, no. 1, pp. 35–41, 2003.

[39] <https://highperformancemachinery.com/yahoo_site_admin/assets/docs/Surface_Finish_Charts.270113339.pdf>

[40] <www.delta-mold.com/FTP/VDI%203400%20Surface%20Finish%20Grade%20Definition.pdf>

[41] G. Schuetz, *Quality Gaging Tips*, Modern Machine Shop, Hanser Pub Inc, 2006.

[42] E. Sancaktar, R. Gomatam, "A study on the effects of surface roughness on the strength of single lap joints," *Journal of Adhesion Science and Technology*, vol. 15, no. 1, 2001.

[43] K. Scott, *Sustainable and Green Electrochemical Science & Technology*, Hoboken: Wiley, 2017.

[44] P. Vermeiren, W. Adriansens, J. Moreels, R. Leysen, "Evaluation of the Zirfon® separator for use in alkaline water electrolysis and Ni-$H_2$ batteries," *International Journal of Hydrogen Energy*, vol. 23, no. 5, pp. 321–324, 1998.